OPEN

Reliable Long-Term Serial Evaluation of Cochlear Function Using Pulsed Distortion-Product Otoacoustic Emissions: Analyzing Levels and Pressure Time Courses

Katharina Bader,[1] Ernst Dalhoff,[2] Linda Dierkes,[1,2] Lore Helene Braun,[3] Anthony W. Gummer,[2] and Dennis Zelle[2,4]

Objectives: To date, there is no international standard on how to use distortion-product otoacoustic emissions (DPOAEs) in serial measurements to accurately detect changes in the function of the cochlear amplifier due, for example, to ototoxic therapies, occupational noise, or the development of regenerative therapies. The use of clinically established standard DPOAE protocols for serial monitoring programs appears to be hampered by multiple factors, including probe placement and calibration effects, signal-processing complexities associated with multiple sites of emission generation as well as suboptimal selection of stimulus parameters.

Design: Pulsed DPOAEs were measured seven times within 3 months for f_2 = 1 to 14 kHz and L_2 = 25 to 80 dB SPL in 20 ears of 10 healthy participants with normal hearing (mean age = 32.1 ± 9.7 years). L_1 values were computed from individual optimal-path parameters derived from the corresponding individual DPOAE level map in the first test session. Three different DPOAE metrics for evaluating the functional state of the cochlear amplifier were investigated with respect to their test-retest reliability: (1) the interference-free, nonlinear-distortion component level (L_{0D}), (2) the time course of the DPOAE-envelope levels, $L_{DP}(t)$, and (3) the squared, zero-lag correlation coefficient (r^2) between the time courses of the DPOAE-envelope pressures, $p_{DP}(t)$, measured in two sessions. The latter two metrics include the two main DPOAE components and their state of interference.

Results: Collated over all sessions and frequencies, the median absolute difference for L_{0D} was 1.93 dB and for $L_{DP}(t)$ was 2.52 dB; the median of r^2 was 0.988. For the low (f_2 = 1 to 3 kHz), mid (f_2 = 4 to 9 kHz), and high (f_2 = 10 to 14 kHz) frequency ranges, the test-retest reliability of L_{0D} increased with increasing signal to noise ratio (SNR).

Conclusions: On the basis of the knowledge gained from this study on the test-retest reliability of pulsed DPOAE signals and the current literature, we propose a DPOAE protocol for future serial monitoring applications that takes into account the following factors: (1) separation of DPOAE components, (2) use of individually optimal stimulus parameters, (3) SNR of at least 15 dB, (4) accurate pressure calibration, (5) consideration of frequency- and level-dependent test-retest reliabilities and corresponding reference ranges, and (6) stimulus levels L_2 that are as low as possible with sufficient SNR to capture the nonlinear functional state of the cochlear amplifier operating at its highest gain.

Key words: Cochlear amplifier, DPOAE components, Ototoxicity, Serial monitoring, Source unmixing, Test-retest reliability, Time domain.

(Ear & Hearing 2024;45;1326–1338)

INTRODUCTION

Distortion-product otoacoustic emissions (DPOAEs) are commonly considered to objectively probe the functional state of the cochlear amplifier, with the outer hair cells (OHCs) regarded as its key element (Brownell 1990; Avan et al. 2013). One important clinical application of DPOAEs is the detection of relative intra-subject changes in OHC function over time during ototoxic therapy (Stavroulaki et al. 2001; Reavis et al. 2011; Poling et al. 2019). Furthermore, serial monitoring of DPOAE changes might also become increasingly relevant for the investigation of putative functional improvements due to pharmacologic intervention or in the development of regenerative therapies in patients with impaired hearing due to OHC loss (Schilder et al. 2019; Shibata et al. 2020).

In clinical practice, the assessment of the state of OHC function by means of the most prominent DPOAE at the cubic difference frequency, $f_{DP} = 2f_1 - f_2$, relies on acoustic stimulation with two continuously presented stimulus tones, with the ratio between the two stimulus frequencies f_1 and f_2 being typically $f_2/f_1 = 1.2$. Conventional paradigms record only a limited number of DPOAE levels at five to seven audiometric frequencies in the range of f_2 = 1 to 8 kHz, using either a fixed stimulus-level difference such as $L_1 = L_2$ or $L_1 - L_2 = 10$ dB, and moderate stimulus levels of $L \geq 55$ dB SPL (Beattie et al. 2003; Petersen et al. 2017; Go et al. 2019; Konrad-Martin et al. 2020), or a pre-defined frequency-independent linear relationship between L_2 and L_1; for example, the scissors paradigm (Kummer et al. 1998; Abdala et al. 2021; Keshishzadeh et al. 2021). However, the knowledge gained from clinically established, standard DPOAE protocols for serial monitoring programs may be limited by multiple factors, including probe placement and calibration effects, signal-processing complexities associated with multiple sites of emission generation as well as the selection of suboptimal stimulus parameters.

With respect to multiple generation sites, conventional paradigms using continuous stimulus tones do not correct for wave interference between the nonlinear-distortion component that arises at or near the f_2-tonotopic place and the coherent-reflection component from the f_{DP}-tonotopic region, but

[1]Department of Otolaryngology, Head and Neck Surgery, Eberhard-Karls-University Tübingen, Tübingen, Germany; [2]Section of Physiological Acoustics and Communication, Department of Otolaryngology, Eberhard-Karls-University Tübingen, Tübingen, Germany; [3]Department of Radiooncology, Eberhard-Karls-University Tübingen, Tübingen, Germany; and [4]Earlab GmbH, Tübingen, Germany.

Supplemental digital content is available for this article. Direct URL citations appear in the printed text and are provided in the HTML and text of this article on the journal's Web site (www.ear-hearing.com).

<zdoi; 10.1097/AUD.0000000000001522>

effectively measure the phasor sum of the waves emerging from the two generation sites (Shera & Guinan 1999). Therefore, depending on the relative phases and levels of the two components, the assessment of cochlear function near the f_2-tonotopic place might lead to an erroneous conclusion (Heitmann et al. 1998; Mauermann & Kollmeier 2004; Dalhoff et al. 2013). For example, destructive interference may cause a considerable reduction in the DPOAE level and, thus, lead to the erroneous conclusion that the cochlear amplifier is nonfunctional near the f_2-tonotopic place. In an analogous manner, a decrease in level of the coherent-reflection component might not be expressed as a decrease in DPOAE level (Zelle et al. 2017c). While, in general, wave interference might not necessarily reduce test-retest reliability, it increases the impact of noise sources in the case of destructive interference due to a reduced signal to noise ratio (SNR) and introduces ambiguity when relating changes in DPOAE level to hearing loss or dysfunction of the cochlear amplifier (Garasto et al. 2023). Furthermore, the two components have been shown to exhibit different susceptibility to hearing loss (Abdala & Kalluri 2017; Prieve et al. 2020; Abdala et al. 2022). The nonlinear-distortion component and the coherent-reflection component depend differently on gain and tuning, through different phenomena, and in different cochlear regions, with the important difference that only the coherent-reflection source, which is secondary to the nonlinear-distortion source, depends on properties of two regions (Shera & Guinan 1999; Abdala et al. 2022). Overall, this means that correcting for wave interference by removing the coherent-reflection component in the DPOAE signal (or even suppressing it in the cochlea) should improve the statistical significance of a DPOAE level change, potentially allowing more accurate serial monitoring of the functional state of the cochlear amplifier.

With respect to suboptimal stimulus parameters, DPOAE levels show significant dependence on the frequency ratio f_2/f_1 (Dreisbach & Siegel 2001; Christensen et al. 2015; Mills et al. 2021; Durante et al. 2022; Stiepan et al. 2022) and the stimulus-level difference $L_1 - L_2$ (Kummer et al. 2000; Zelle et al. 2015), both of which feature frequency-specific optimum values that increase sensitivity for detecting damage to the cochlear amplifier (Whitehead et al. 1995; Kummer et al. 1998; Zelle et al. 2020). Moreover, stimulus-level parameters optimized for sensitivity might not necessarily reflect the optimum condition for serial monitoring of cochlear impairments. For example, lower stimulus levels increase the sensitivity for detecting hearing loss (Johnson et al. 2010; Rao & Long 2011), but then require longer averaging time to counteract the increased influence of noise sources due to lower DPOAE levels. However, optimum frequency-dependent stimulus settings are rarely considered in conventional DPOAE protocols.

Moreover, the frequencies of interest incorporated in the DPOAE protocol depend on the type of serial monitoring. For example, ototoxic therapies often, but not always, initially result in damage to the basal cochlea (Laurell & Bagger-Sjöbäck 1991), which manifests as high-frequency hearing loss (Fausti et al. 2003; Reavis et al. 2011). Therefore, the ideal measurement protocol should support DPOAE acquisition over a wide range of frequencies, including those well above 8 kHz (Poling et al. 2019).

In hearing research, during the past two decades, alternative and more complex stimulation and recording techniques have been developed with the intent of reducing wave interference (Heitmann et al. 1998; Kalluri & Shera 2001; Long et al. 2008; Moleti et al. 2012; Dalhoff et al. 2013; Abdala et al. 2015), optimizing DPOAE generation and sensitivity (Zelle et al. 2017c, 2020), improving high-frequency calibration procedures (Dreisbach et al. 2018; Maxim et al. 2019; Poling et al. 2019; Abdala et al. 2022), and possibly revealing new diagnostic information about the state of cochlear mechanics (Moleti et al. 2005; Abdala et al. 2021).

Here, we evaluate the test-retest reliability of short-pulse DPOAE time signals recorded at individually identified optimal stimulus levels for frequencies between f_2 = 1 and 14 kHz to investigate the test-retest reliability of (1) the DPOAE nonlinear-distortion component level L_{OD}, (2) the time course of the DPOAE-envelope levels $L_{DP}(t)$, and (3) the squared, zero-lag correlation coefficient (r^2) between the time courses of the DPOAE-envelope pressures from two measurement sessions. The latter two parameters are an indicator of the repeatability of the temporal structure of the DPOAE signal, including both the nonlinear-distortion and coherent-reflection components.

MATERIAL AND METHODS

Subjects and Study Design

Short-pulse DPOAE time signals analyzed here originate from experiments of an earlier published study by the authors (Bader et al. 2021), which compared the test-retest reliability of estimated distortion-product thresholds (EDPTs) to that of behavioral thresholds. While the previous study focused on the definition of a baseline for the test-retest reliability of a quantitative assessment of hearing impairment using EDPTs (Boege & Janssen 2002; Gorga et al. 2003; Zelle et al. 2017c) derived from the DPOAE growth behavior in L_1, L_2 space (Whitehead et al. 1995; Kummer et al. 2000; Zelle et al. 2020), the present study aims to quantify the intra-subject test-retest reliabilities of the level of the nonlinear-distortion component and the temporal structure of DPOAE signals. Their test-retest reliability may be of interest in tailored serial monitoring applications focusing solely on the integrity of the cochlear amplifier, especially since the time course of the signal incorporates information about both the distortion-generation and the reflection mechanisms that form the overall DPOAE response (Shera & Guinan 1999).

Short-pulse DPOAEs were recorded bilaterally in 10 healthy, normal-hearing (four-pure-tone average, 0.5, 1, 2, 4 kHz <20 dB HL; Fig. 1) subjects (mean age = 32.1 ± 9.7 years; six female and four male subjects) in a total of seven test sessions distributed across 3 months. To ascertain the stability of the hearing status throughout the experimental series, each session included otoscopy by an ENT specialist (KB), tympanometry (Madsen-Zodiac 901, GN Otometrics, Münster Germany; Sentiero SD07, Path Medical GmbH, Germering, Germany) and pure-tone audiometry (0.25 to 16 kHz; Audiometer AT 900 or AT 1000, Auritec, Medizindiagnostische Systeme, Hamburg, Germany). Exclusion criteria regarding otoscopy and tympanometry were pathological changes of the tympanic membrane or middle ear, such as seromucotympanum, cerumen, sclerotic plaques, atrophic tympanic membrane, or perforations. The tympanometry recorded the maximum change in compliance for a frequency of 226 Hz and pressure between 300 and −300 mmH_2O. To be included in the study, the tympanogram had to be type A according to Jerger (1970) and present a peak pressure above −65 daPa. Both ears were investigated. The Ethics Committee of

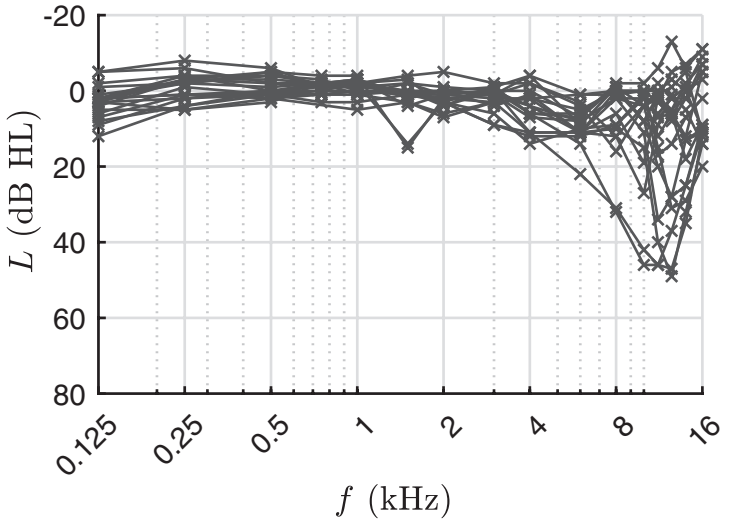

Fig. 1. Behavioral thresholds of all included (4 PTA, 0.5, 1, 2, 4 kHz <20 dB HL) ears (N = 20) recorded in the first test session by PTA. PTA indicates pure-tone audiometry.

the University of Tübingen approved the study (265/2018B01), which was conducted in accordance with the Declaration of Helsinki for human experiments. The interested reader is referred to Bader et al. (2021) for an elaborated description of the study design and measurement procedures.

DPOAE Acquisition

Measurement System and Calibration • Simultaneous bilateral recording of DPOAEs was performed using an ER-10C DPOAE ear probe (Etymotic Research, Elk Grove Village, IL, USA) controlled by custom-built instrumentation software (LabVIEW Version 17.0, National Instruments, Austin, TX, USA) via data acquisition cards (NI PCI 6733, NI PCI 4472, National Instruments, Austin, TX, USA). Automated DPOAE signal analysis was performed in MATLAB (Version 9.6, The MathWorks, Natick, MA, USA). To achieve a similar position of the ear probe across sessions, the frequency response of the ear-canal sound pressure from 0.3 to 20 kHz was determined before the calibration and the amplitude and phase responses visually compared with those of the previous recordings. If deemed necessary, the ear-probe fit was re-adjusted by the investigator before continuing with the calibration and recording procedures, with the aim of approximately replicating the position of any resonances with respect to frequency. In the post-hoc analysis, it was evident that an antiresonance, typically apparent between 8 and 12 kHz, did not shift by more than 500 Hz across the seven examinations. The resultant level differences amounted to at most 10 dB, indicating that our procedure reduced, but did not entirely remove, calibration differences due to varying probe positions. The stimulus sound pressure was calibrated using in-ear calibration of the speakers before each session. A detailed description of the calibration technique is given elsewhere (Zelle et al. 2015; Bader et al. 2021).

Short-Pulse DPOAE Acquisition • DPOAE signals were recorded at 10 L_2 values for 14 frequency pairs in the range of f_2 = 1 to 14 kHz (f_2/f_1 = 1.2). Frequency-specific stimulus levels started at L_2 = 25 dB SPL for $f_2 \leq$ 3 kHz, 30 dB SPL for 4 $\leq f_2 \leq$ 9 kHz, and 35 dB SPL for $f_2 >$ 9 kHz, and increased by 5-dB steps. On the basis of the linear relationship $L_1 = aL_2 + b$ introduced by Kummer et al. (1998) for choosing L_1 for a given L_2, in our experiments a and b were derived for each ear and each f_2 (Zelle et al. 2020). These individually chosen, frequency-dependent values for a and b resulted in stimulus-level pairs that are designed to maximize the amplitudes of the nonlinear-distortion components and, therefore, are considered optimal (Zelle et al. 2020). These individually optimal values were derived during the first measurement session, directly from the growth behavior of 21 amplitudes of the nonlinear-distortion component plotted in L_1, L_2 space for each frequency, depending on their SNR. This representation of amplitude as function of L_1 and L_2 yields so-called DPOAE level maps (Zelle et al. 2020). If a level map was not available for a given frequency, for example, due to an insufficient number of DPOAEs complying with the SNR threshold of 10 dB, the frequency-specific optimal-path parameters from Zelle et al. (2015) were used.

The acquisition of short-pulse DPOAEs utilizes short stimulus pulses that facilitate the separation of the nonlinear-distortion and coherent-reflection components in the time domain due to their different latencies. The f_1 pulses had a duration between 20 and 40 ms, depending on stimulus frequency. During the steady state of each f_1 pulse, an f_2 pulse was presented with a frequency-specific full-width-at-half-maximum between 3.27 ms for $f_2 \geq$ 4 kHz and 13.07 ms at f_2 = 1 kHz. The length of the f_2 pulses was chosen to be commensurate with the expected relative delay between the two main DPOAE components (Zelle et al. 2017c; Bader et al. 2021). Figure 2 shows a short-pulse DPOAE response at f_2 = 2 kHz with the envelopes of the stimulus pulses depicted at the bottom (red lines). To reduce measurement time, the stimulus pulse pairs were concatenated into pulse trains with a 1-ms pause between the longer f_1 pulses and a 2-ms pause before the first and after the last f_1 pulse (Zelle et al. 2020). The acquisition of 14 DPOAEs for 14 stimulus frequencies required two pulse trains, each with a total duration of 180 ms and composed of seven pulse pairs associated with seven f_2 frequencies. Pulse trains were presented simultaneously to both ears, but the order of the frequencies within a train was opposite in the two ears to avoid (efferent) suppression effects that might occur had the frequency order been the same in both ears. The light-gray lines at the bottom of Figure 2 show the

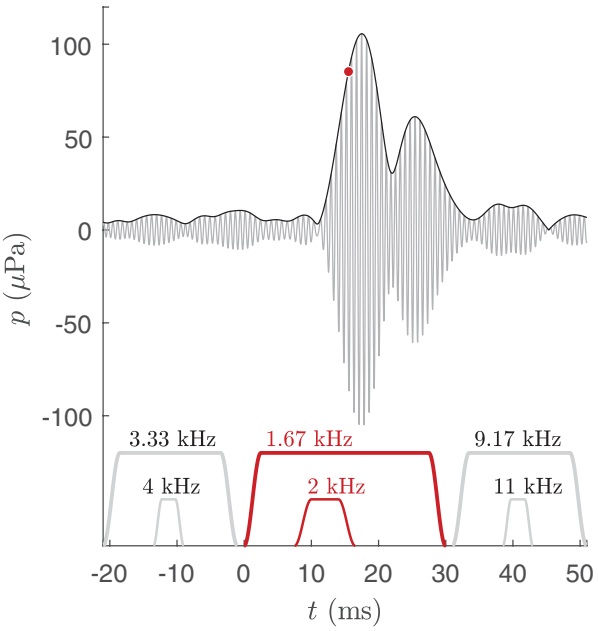

Fig. 2. DPOAE time signal in response to short-pulse stimulation. Time signal (gray lines) and envelope (dark-gray lines) of a short-pulse DPOAE signal recorded from ear S163R at f_2 = 2 kHz, L_2 = 45 dB SPL, L_1 = 57 dB SPL. Bandpass filtering extracted the DPOAE signal from the multi-frequency recording that comprises multiple DPOAEs elicited by pulse trains. Red dot: amplitude of the nonlinear-distortion component estimated with onset decomposition. Due to their different latencies, the two components of the DPOAE signal become distinguishable in the time domain, with the coherent-reflection component following the nonlinear-distortion component. Red lines at the bottom: shape and arrangement of the f_1 and f_2 stimulus pulses that evoked the DPOAE signal. Bold light-gray lines: pulses in the multi-frequency pulse train that evoke a DPOAE at f_2 = 4 and 11 kHz, respectively (responses not shown). In this example, the first peak of the DPOAE time signal represents the nonlinear-distortion component, the second peak is the coherent-reflection component, and the intervening dip is the state of destructive interference. Therefore, the temporal structure of the DPOAE signal contains several items of information about the functionality of the cochlear amplifier. DPOAE indicates distortion-product otoacoustic emission.

stimulus pulses in the pulse-train arrangement that were used to evoke DPOAE responses before (f_2 = 4 kHz) and after (f_2 = 11 kHz) that shown in the figure (f_2 = 2 kHz). Each bilateral recording composed of seven different stimulus frequencies was averaged until an SNR of at least 10 dB for all DPOAEs or a maximum of 100 repetitions was reached. Measurement blocks with excessive noise or motion artifacts and, therefore, not yielding an increase of SNR with subsequent presentations, were automatically excluded from the averaging process by the analysis software. Primary-tone phase variation was used to cancel the stimulus pulses after ensemble averaging by shifting the phases of the f_1 and f_2 pulses in subsequent segments by 90° and 180°, respectively (Whitehead et al. 1996). The total maximum recording time for all short-pulse DPOAEs at 14 frequencies with 10 levels in both ears was 6 min; that is, 18 s per pulse train or about 2.6 s per single frequency-level combination.

Analysis of DPOAE Time Responses • Each averaged recording comprised seven DPOAE signals with stimulus frequencies depending on the particular multi-frequency pulse train. Bandpass filtering around the DPOAE frequency and bandwidths commensurate with the half width of the corresponding f_2 stimulus pulse yielded the DPOAE time responses. An automated signal-detection algorithm (Zelle et al. 2017b, c) determined the beginning and the interval of the DPOAE signal; this interval includes both DPOAE components. The detected DPOAE time signal was considered statistically significant if its variance was significantly higher than that of the superimposed noise at a significance level of $\alpha = 0.05$ (χ^2 test). In addition, all valid signals with a time delay of less than 500 µs between the onsets of the f_2 pulse and the DPOAE were considered as possible technical distortion from the experimental system (e.g., from the ear probe) and excluded from further analysis.

Due to their different latencies, the DPOAE components become distinguishable in their time course (Fig. 2), with the nonlinear-distortion component arising before the coherent-reflection component emerges. The nonlinear-distortion component dominates the DPOAE response for a short time period, which relates to the relative delay between the two DPOAE components. They become directly separable in the time domain when the duration of the f_2 stimulus pulse corresponds approximately to the relative delay between the nonlinear-distortion and the coherent-reflection components. To extract the amplitude of the nonlinear-distortion component, the envelope of the DPOAE time signal was automatically sampled at a time point between the DPOAE onset and the onset of the coherent-reflection component, accounting for the varying latency of the DPOAE signal and its components as a function of frequency, level, and integrity of the cochlea. This amplitude is denoted by P_{OD}, where the subscript "OD" is used to emphasize that the automated extraction process (Zelle et al. 2017b) is based on onset decomposition (Vetešník et al. 2009). P_{OD} was converted to the level L_{OD}, which in turn was accepted for statistical analysis if its SNR was at least 10 dB.

In addition to being able to extract the nonlinear-distortion component directly in the time domain, the acquisition of short-pulse DPOAEs provides the advantage of analyzing and comparing the time course of DPOAE signals across various measurement sessions. Therefore, an SNR-based threshold detection algorithm, that accepts samples of the DPOAE-envelope exhibiting an SNR ≥ 6 dB, was used to obtain an estimate of the signal offset of each DPOAE signal. The detected signal onset and offset span an interval in the time signal $p(t)$ that is dominated by the DPOAE signal $p_{DP}(t)$, which—provided the SNR is sufficiently high—includes both the nonlinear-distortion and the coherent-reflection components (Fig. 3, black lines). This time-interval estimate is required for calculating metrics associated with the time courses of the DPOAE signals across measurement sessions (see Statistics).

Statistics

SPSS Statistics software (version 26, IBM, New York, USA) was used for statistical testing. To quantify intra-subject test-retest reliability of L_{OD}, two different metrics were used: (1) absolute differences (ADs) between test and retest sessions (1 versus 2, 1 versus 3, 1 versus 4,..., 2 versus 3, 2 versus 4,...; N = 21), and (2) the intraclass-correlation coefficient (two-way mixed, absolute consistency). Intra-subject test-retest reliability determines the ability of one method to provide similar results

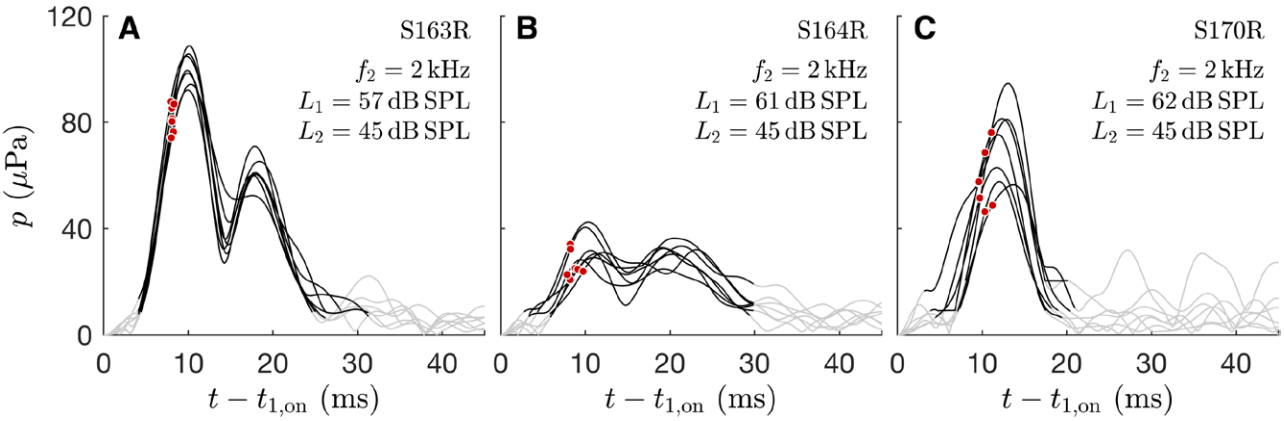

Fig. 3. Comparison of test-retest reliability of DPOAE signals in three different ears at L_2 = 45 dB SPL. In each panel, one DPOAE response is shown for each of the seven sessions. Gray lines: Envelope of recorded and filtered signal. Black lines: Interval with detected DPOAE signal. Red dots: estimate of the amplitude of the nonlinear-distortion component, based on the onset-decomposition technique. A, The time course of the DPOAE signal suggests destructive interference between the two DPOAE components. The total time course—the part dominated by the nonlinear-distortion component, the part dominated by the interference, and the part dominated by the coherent-reflection component—show high stability. B, The DPOAE signal amplitude is much lower than for the subject in A, which may indicate that the noise has a greater impact on test-retest reliability. Moreover, the DPOAE time courses dominated by the nonlinear-distortion component on the one hand and the coherent-reflection component on the other hand show similar amplitudes. If the components were in phase opposition, they would approximately mutually cancel, preventing source separation. C, A DPOAE signal without clearly visible coherent-reflection component. Median absolute differences (see Statistics for definitions): 0.67 dB (A), 1.66 dB (B), 1.57 dB (C) for L_{OD}; 1.26 dB (A), 2.47 dB (B), 3.06 dB (C) for $L_{DP}(t)$. Median, squared zero-lag correlation coefficient r^2 for $p_{DP}(t)$: 0.991 (A), 0.959 (B), 0.963 (C). Strikingly, in all three cases, r^2 is exceedingly high (≥ 0.96). DPOAE indicates distortion-product otoacoustic emission.

when repeated for the same subject under the same experimental conditions (cf. Fig. 3).

Moreover, the acquisition of short-pulse DPOAE time signals allows quantification of the intra-subject test-retest reliability of the time course of the DPOAE signal between test and retest sessions. For this purpose, we used the time course of the DPOAE-envelope pressures $p_{DP}(t)$ as well as the time course of the DPOAE-envelope levels $L_{DP}(t)$. To objectively quantify the differences between two DPOAE responses, two further metrics were used to compare all samples of $p_{DP}(t)$ that exhibit an SNR ≥ 6 dB: (1) the squared, zero-lag correlation coefficient (r^2) between the $p_{DP}(t)$ from two sessions, and (2) the mean value of the sample-wise ADs between the $L_{DP}(t)$ from two sessions. In contrast with the interference-free, nonlinear-distortion component level, L_{OD}, which is a metric evaluated at a single time instant, the mean value of the sample-wise ADs and r^2 consider the time signal of the DPOAE response.

Statistical significance between samples of ADs (see Supplementary Figure 1 in Supplemental Digital Content, http://links.lww.com/EANDH/B412, for histograms of relative and ADs of L_{OD}, respectively) was tested using the Mann–Whitney U test to compare the distribution of two samples, and the Kruskal–Wallis test to compare the distribution of multiple samples.

RESULTS

For f_2 = 1 to 14 kHz, 9706 out of 19,600 DPOAE recordings (49.5%) yielded reliable short-pulse DPOAEs (Supplementary Table 1 in Supplemental Digital Content, http://links.lww.com/EANDH/B413).

Dependence on f_2

Figure 4 shows as a function of f_2 (1) the ADs of the level of the nonlinear-distortion component L_{OD}, (2) the mean sample-wise ADs of the time course of the DPOAE-envelope levels $L_{DP}(t)$, and (3) the squared, zero-lag correlation coefficient, r^2, between two-time courses of the DPOAE-envelope pressures. For L_{OD} and $L_{DP}(t)$, statistical data are displayed as boxplots of median and interquartile range (IQR). The upper error bars represent a range that covers 90% of the data starting from a minimum value of AD of 0 dB. For r^2, the dots and arrow heads indicate the median values and the IQR, while the lower error bars represent a range that encompasses 90% of the data descending from a maximum value of r^2 = 1. Data are collated from the 21 pairwise combinations of the seven sessions. Table 1 presents the data from Figure 4 in tabular form. Table 2 presents the intraclass-correlation coefficient for L_{OD} at each f_2 = 1 to 14 kHz.

The test-retest reliabilities of L_{OD}, $L_{DP}(t)$, and r^2 were dependent on stimulus frequency with significant differences between individual frequencies (Kruskal–Wallis test: L_{OD}, N = 24,497, $p < 0.001$; $L_{DP}(t)$, N = 24,497, $p < 0.001$; r^2, N = 24,497, $p < 0.001$). For all frequencies f_2 = 1 to 14 kHz, the median AD was 1.93 dB (IQR = 2.85 dB) for L_{OD} and 2.52 dB for $L_{DP}(t)$ (IQR = 2.02 dB); the median of r^2 was 0.988 (IQR = 0.022).

To further analyze the dependency of the test-retest reliabilities of L_{OD}, $L_{DP}(t)$, and r^2 on f_2, the data were divided into three frequency ranges, f_2 = 1 to 3 kHz, f_2 = 4 to 10 kHz, and f_2 = 11 to 14 kHz. At low frequencies (f_2 = 1 to 3 kHz), L_{OD} exhibited higher test-retest reliability, with median ADs ranging between 1.21 and 1.48 dB, than at mid frequencies (f_2 = 4 to 10 kHz) or high frequencies (f_2 = 11 to 14 kHz) with median ADs ranging between 1.89 dB for f_2 = 13 kHz and 3.05 dB for f_2 = 10 kHz. Significant differences in the test-retest reliability of 1.03 dB between the low-frequency and mid-frequency ranges (Mann–Whitney U test, $z = -35.86$, $p < 0.001$) and of 1.05 dB between the low- and high-frequency ranges (Mann–Whitney U test, $z = 24.88$, $p < 0.001$) were observed. Between the mid- and

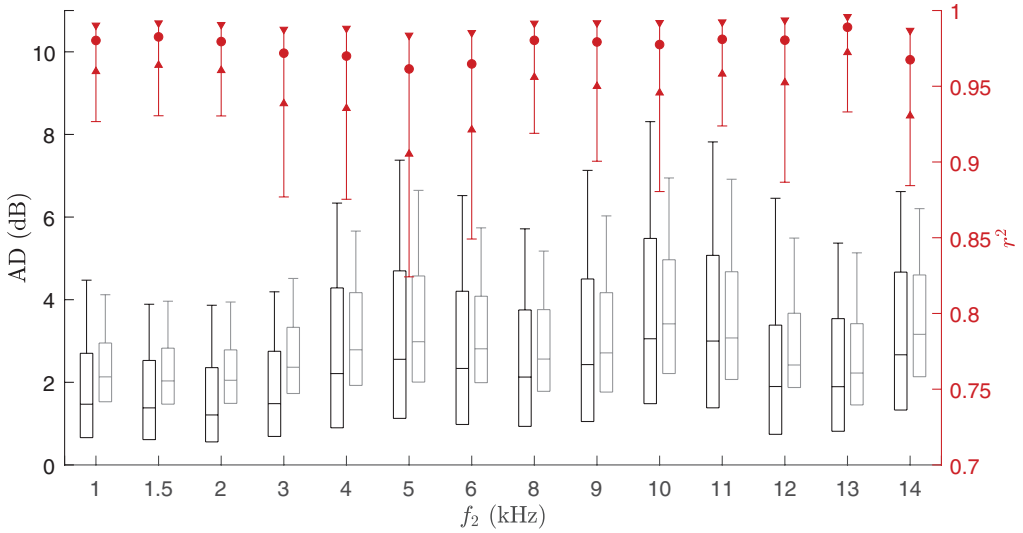

Fig. 4. Dependence of test-retest reliability of short-pulse DPOAEs on f_2, collated across all subjects and the 21 pairwise combinations of seven sessions. Metrics are (1) the level of the nonlinear-distortion component, L_{OD} (black), (2) the time course of the DPOAE-envelope levels, $L_{DP}(t)$ (gray), and (3) the squared, zero-lag correlation coefficient between two time courses of the DPOAE-envelope pressures, r^2 (red). Test-retest reliability of L_{OD} and $L_{DP}(t)$ are presented as AD. Boxes: median and IQR from the first to the third quartile. Upper error bars: 90th percentile indicating a range that covers 90% of the ADs starting from AD = 0. For r^2, box plots are presented as arrowheads directed to the median (dots). Lower error bars: 10th percentile indicating a range that covers 90% of r^2 starting from r^2 = 1. AD indicates absolute differences; DPOAE, distortion-product otoacoustic emission; IQR, interquartile range.

high-frequency ranges, a significant difference (0.02 dB) was not observed (Mann–Whitney U test, $z = 1.06$, $p = 0.289$). For $f_2 = 1$ to 3 kHz, median AD 1.38 dB, IQR 1.97 dB, 90%-range 4.11 dB, N = 9374; for $f_2 = 4$ to 10 kHz, median AD 2.41 dB, IQR 3.40 dB, 90%-range 6.84 dB, N = 12,102; for $f_2 = 11$ to 14 kHz, median AD 2.43 dB, IQR 3.33 dB, 90%-range 6.84 dB; N = 3021.

Similar trends were observed for the time course of DPOAE-envelope levels $L_{DP}(t)$; there was a 0.7-dB improvement in test-retest reliability for the 1 to 3 kHz frequency range compared with the mid- or high-frequency ranges ($f_2 = 1$ to 3 kHz, median AD = 2.14 dB, IQR = 1.44 dB, 90%-range = 4.15 dB, N = 9374; $f_2 = 4$ to 10 kHz, median AD = 2.86 dB, IQR = 2.34 dB, 90%-range = 6.04 dB, N = 12,099; $f_2 = 11$ to 14 kHz, median AD = 2.80 dB, IQR = 2.40 dB, 90%-range = 6.21 dB; N = 3021).

The time course of the DPOAE-envelope pressure showed higher test-retest reliability, as ascertained with r^2, for the low- and the high-frequency ranges compared with the mid-frequency range ($f_2 = 1$ to 3 kHz, median $r^2 = 0.979$, IQR = 0.03, 90%-range = 0.915, N = 9374; $f_2 = 4$ to 10 kHz, median $r^2 = 0.947$, IQR = 0.05, 90%-range = 0.866, N = 12,099; $f_2 = 11$ to 14 kHz, median $r^2 = 0.982$, IQR = 0.04, 90%-range = 0.918, N = 3021).

Dependence on L_2

To evaluate the potential effect of stimulus level L_2 on test-retest reliability, Figure 5 presents the median ADs for L_{OD} (A) and $L_{DP}(t)$ (B) as well as the median of r^2 (C) for L_2 and f_2. For f_2

TABLE 1. Dependence of test-retest reliability of short-pulse DPOAEs on f_2 collated across all subjects and the 21 pairwise combinations of seven sessions

	L_{OD}			$L_{DP}(t)$			r^2			
f_2 (kHz)	AD Median	AD IQR	AD 90%	AD Median	AD IQR	AD 90%	Median	IQR	90%	N
1	1.47	2.04	4.48	2.13	1.42	4.12	0.980	0.030	0.926	1820
1.5	1.38	1.92	3.89	2.03	1.36	3.96	0.983	0.028	0.930	2707
2	1.21	1.80	3.87	2.05	1.30	3.94	0.980	0.030	0.930	2323
3	1.48	2.06	4.19	2.36	1.60	4.52	0.972	0.049	0.877	2524
4	2.21	3.39	6.34	2.79	2.25	5.66	0.970	0.053	0.875	2667
5	2.56	3.57	7.38	2.98	2.57	6.65	0.961	0.078	0.824	2557
6	2.34	3.22	6.52	2.81	2.09	5.74	0.965	0.064	0.849	2354
8	2.13	2.82	5.72	2.56	1.98	5.18	0.980	0.036	0.919	1568
9	2.43	3.45	7.14	2.71	2.41	6.03	0.979	0.042	0.900	1521
10	3.05	4.00	8.32	3.42	2.75	6.95	0.978	0.046	0.880	1435
11	3.00	3.69	7.82	3.07	2.61	6.92	0.981	0.034	0.924	1316
12	1.90	2.64	6.55	2.42	1.80	5.54	0.980	0.041	0.887	85
13	1.89	2.73	5.37	2.22	1.97	5.14	0.989	0.024	0.933	1029
14	2.67	3.34	6.62	3.16	2.46	6.21	0.968	0.056	0.884	591
Total$_{1–14\ kHz}$	1.93	2.85	5.96	2.52	2.02	5.44	0.988	0.022	0.944	24,497

The entries correspond to the data presented graphically in Figure 4. N denotes the total number of underlying pairs of comparisons at each frequency. AD has units of dB.
AD, absolute differences; DPOAE, distortion-product otoacoustic emission; IQR, interquartile range.

TABLE 2. Test-retest reliability of L_{OD} quantified with the ICC and the 95% CI for each f_2

	L_{OD}			
f_2 (kHz)	ICC	95% CI		N
1	0.955	0.933	0.972	47
1.5	0.967	0.956	0.976	92
2	0.985	0.980	0.990	79
3	0.974	0.964	0.981	83
4	0.945	0.926	0.961	89
5	0.945	0.926	0.961	92
6	0.962	0.948	0.973	87
8	0.967	0.950	0.980	47
9	0.957	0.929	0.975	47
10	0.899	0.840	0.942	38
11	0.958	0.925	0.980	23
12	0.936	0.892	0.966	30
13	0.971	0.949	0.986	25
14	0.945	0.866	0.984	10
$\text{Total}_{1–14\ kHz}$	0.974	0.971	0.977	789

N denotes the number of underlying values for the ICC, when DPOAEs were measured and accepted within an ear for a given stimulus level pair in all seven sessions (out of a maximum of 200 = 20 ears × 10 stimulus level pairs).

CI, confidence interval; DPOAES, distortion-product otoacoustic emissions; ICC, intraclass-correlation coefficient.

≤ 3 kHz, the test-retest reliability of $L_{DP}(t)$ tended to be independent of L_2, whereas for decreasing L_2 the test-retest reliability of L_{OD} and r^2 both tended to decrease. For $f_2 > 3$ kHz, a consistent dependence of test-retest reliability of L_{OD} and $L_{DP}(t)$ on L_2 was not found, whereas the test-retest reliability of r^2 decreased at lower L_2 up to about 11 kHz. For all three metrics, a consistent dependence of test-retest reliability on L_2 was not found for $f_2 > 11$ kHz.

Dependence on SNR

The dependence of test-retest reliability on SNR can be accurately derived from the level L_{OD} of the nonlinear-distortion component that was sampled at a single time point before the coherent-reflection component builds up. In contrast, the DPOAE time course represented by the metrics $L_{DP}(t)$ and r^2, both of which are calculated from $p_{DP}(t)$, exhibit a time-variant SNR due to the varying amplitude of the DPOAE time course. To analyze the dependency of the test-retest reliability of L_{OD} on the SNR, ADs were sorted into four SNR groups: group 1, low-SNR DPOAEs with SNR of ≤ 15 dB (N = 2183); group 2, medium-SNR DPOAEs with 15 < SNR ≤ 20 dB (N = 3146); group 3, high-SNR DPOAEs with 20 < SNR ≤ 25 dB (N = 2874); group 4, very-high-SNR DPOAEs with SNR > 25dB (N = 2674). The DPOAE levels were also divided into three frequency groups (f_2 = 1 to 3 kHz, f_2 = 4 to 9 kHz, and f_2 = 10 to 14 kHz). SNR was defined as the difference between the level of the nonlinear-distortion component and the level of the noise. The noise floor was estimated as the root-mean-square of the difference between two subsets of the underlying segments from the DPOAE recording in a 50-ms time-interval centered on the DPOAE response. Figure 6 shows the test-retest reliability of L_{OD} for different SNR and frequency groups presented as boxplots of their ADs. For each frequency group, the test-retest reliability of L_{OD} increased with increasing SNR. The median of ADs decreased from 2.21 to 0.87 dB for f_2 = 1 to 3 kHz, from 3.63 to 1.60 dB for f_2 = 4 to 9 kHz, and from 4.20 to 1.84 dB for f_2 = 10 to 14 kHz.

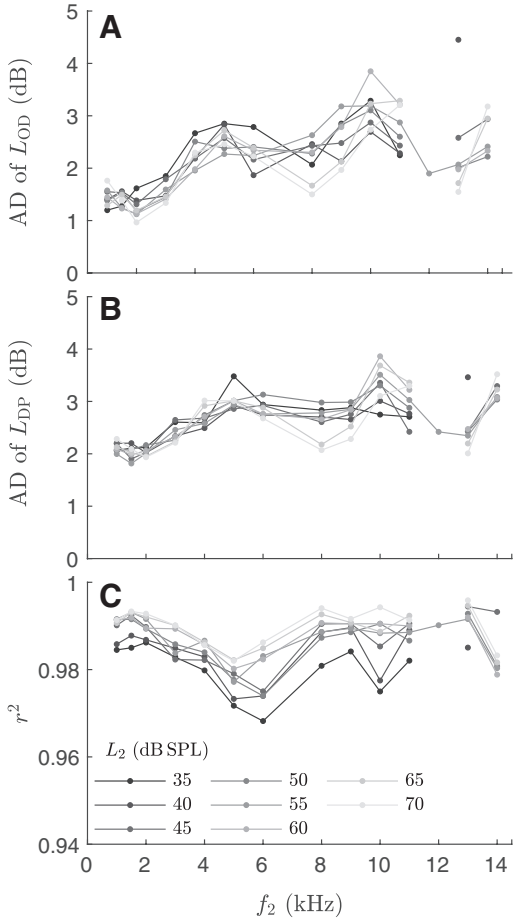

Fig. 5. Dependence of test-retest reliability on L_2, as function of f_2, based on the median AD of L_{OD} (A), the median AD of $L_{DP}(t)$ (B), and the median of r^2. Data have only been included in the figure when there were at least 10 samples available to estimate a median. Notice that the test-retest reliability of the time course of the DPOAE-envelope pressure, as quantified by r^2, is smaller at low stimulus levels and frequencies up to about 11 kHz. AD indicates absolute differences; DPOAE, distortion-product otoacoustic emission.

Additional results (such as mean values of ADs) were computed for comparison with the literature and are given in the Discussion.

DISCUSSION

Three different DPOAE metrics for evaluating the functional state of the cochlear amplifier were investigated with respect to their test-retest reliability. (1) The level of the nonlinear-distortion component L_{OD}, extracted in the time domain using onset decomposition, determines the amplitude of the nonlinear-distortion component at a given time, free of interference, just before the reflection component starts to interfere. (2) The time course of the DPOAE-envelope levels, $L_{DP}(t)$, on the other hand, provides the total time course of the DPOAE signal, including the two main DPOAE components and their state of interference. (3) The squared, zero-lag correlation coefficient (r^2) between time courses of the DPOAE-envelope

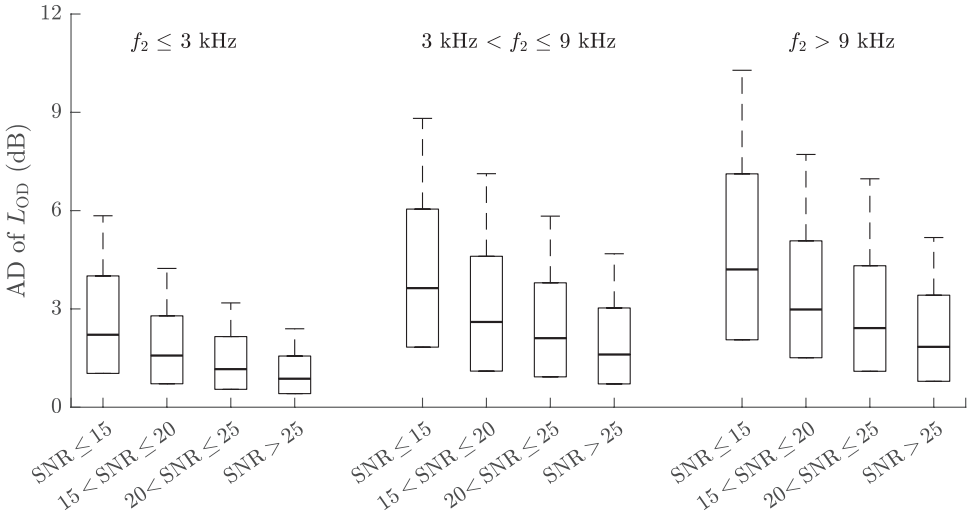

Fig. 6. Dependence of test-retest reliability on the SNR based on the median AD of L_{OD} for three frequency ranges, f_2 = 1–3 kHz (left), f_2 = 4–9 kHz (middle), and f_2 = 10–14 kHz (right), and four SNR ranges. Boxes: median and IQR from the first to the third quartile. Upper error bars: 90% range (cf. Fig. 4). For each frequency range, the test-retest reliability improved with increasing SNR. AD indicates absolute differences; IQR, interquartile range; SNR, signal to noise ratio.

pressures measured in two sessions provides evidence for differences between the time courses of the DPOAE signals, resulting from inter-session differences between the two main DPOAE components and their state and degree of interference. Knowledge of the different DPOAE metrics, their test-retest reliability, and factors influencing their test-retest reliability provides a basis for designing tailored measurement protocols for clinical monitoring applications, such as detecting ototoxicity and its progression.

The test-retest reliability of L_{OD} was found to be in the range of the test-retest reliabilities of DPOAE levels described in the literature. Thus, the extraction of the nonlinear-distortion component of the short-pulse DPOAE signal with onset-decomposition sampling in the time domain was found to be not only a time-efficient and precise (Zelle et al. 2017b, 2020; Bader et al. 2021) but also a stable and highly reliable method. To the best of our knowledge, there are no studies that have investigated the stability of pulsed DPOAE time signals or used DPOAE time courses as a metric for serial measurements.

Sources of Variability in DPOAE Time Signals

Serial monitoring of the functional state of the cochlear amplifier may be based on single DPOAE responses at certain frequencies for certain stimulus conditions. Therefore, it is necessary to know how consistent DPOAEs are over time in the absence of pathology (McMillan 2014). In general, the test-retest reliability of DPOAEs may be influenced by (1) fluctuations in the middle-ear transfer characteristics, (2) inadequate averaging time to reduce the influence of noise, (3) calibration errors, (4) deficiencies in the DPOAE signal-detection algorithm, and (5) fluctuation in the functionality of the cochlear amplifier.

Fluctuations in the middle-ear transfer characteristics can change the amplitude of the DPOAE over time (Avan et al. 2000; Kreitmayer et al. 2019). This confounding factor can be addressed, amongst others, by individual DPOAE level maps that represent the DPOAE amplitude as a function of the stimulus levels L_1 and L_2 and, therefore, automatically account for the middle-ear transfer function. In this study, L_1 values were mainly assigned from individual optimal-path parameters derived from the corresponding individual DPOAE level maps obtained during the first measurement session (Zelle et al. 2020). Therefore, theoretically, some variability could have been due to differences in middle-ear transmission across sessions.

Clearly, increasing the DPOAE level increases the SNR as the contribution of the noise to the DPOAE amplitude becomes negligible and the measured DPOAE level represents the true DPOAE level (Whitehead et al. 1993; Beattie & Ireland 2000). The test-retest reliability of L_{OD} improved consistently with increasing SNR (Fig. 6). This study suggests a minimum SNR of 15 dB for the use of L_{OD} in serial monitoring protocols. Similar recommendations were given in Beattie and Bleech (2000), Wagner et al. (2008), and Keppler et al. (2010). Although a higher SNR is, in principle, associated with higher test-retest reliability, it is important to set moderate limits when establishing a measurement protocol in order to be able to measure DPOAEs in as many patients as possible. High SNR limits would possibly exclude low DPOAE emitters. It would probably be advisable to perform an adaptive screening test before starting the follow-up measurements in order to achieve the maximum SNR values that allow the highest test-retest reliability.

Due to calibration errors, small changes in probe position can result in DPOAE level shifts at frequencies above 2 kHz (Scheperle et al. 2008; Charaziak & Shera 2017). Maxim et al. (2019) compared the effect of conventional SPL-based stimulus calibration, based on the total SPL measured at the probe microphone, and forward-pressure-level (FPL) stimulus calibration, with OAEs expressed in either SPL or emitted pressure level (EPL), on the test-retest reliability. The FPL/EPL calibration approach produces an average improvement in test-retest reliability of 0.5 to 2.0 dB relative to the SPL approach, and DPOAEs with greater intra-subject variability are associated with stronger FPL/EPL benefits (Maxim et al. 2019). The use of in-the-ear pressure calibration for the short-pulse acquisition in the present study, instead of an FPL stimulus calibration technique with DPOAEs expressed in EPL, represents a limiting factor. For

f_2 = 1 to 14 kHz, a moderate correlation between the ADs of L_{OD} and of calibrated SPLs was detected (Spearman's correlation coefficient $r = 0.303$, $p < 0.001$, N = 27,481). Dividing the ADs into frequency ranges, we calculated for the lower frequencies f_2 = 1 to 3 kHz a low correlation (Spearman's correlation coefficient $r = 0.130$, $p < 0.001$, N = 9452), for the mid frequencies f_2 = 4 to 10 kHz a moderate correlation (Spearman's correlation coefficient $r = 0.334$, $p < 0.001$, N = 13,573) and for the higher frequencies f_2 = 11 to 14 kHz a rather low to moderate correlation (Spearman's correlation coefficient $r = 0.200$, $p < 0.001$, N = 4456). The higher correlation coefficients in the 4 to 14 kHz region might be caused by SPL-calibration errors in our serial measurements, notwithstanding our efforts to maintain similar ear-probe fit transfer functions across probe placements for each test session (see Materials and methods).

Dependence of the Test-Retest Reliability on Stimulus Frequency f_2 and Stimulus Level L_2

At low frequencies, f_2 = 1 to 3 kHz, the test-retest reliabilities of L_{OD} and $L_{DP}(t)$ were significantly better by about 1 dB than those for mid or high frequencies. Similarly, r^2 showed higher test-retest reliability at low frequencies than at mid frequencies. In contrast with L_{OD} and $L_{DP}(t)$ at high frequencies, r^2 showed a relatively high test-retest reliability. Relatively low test-retest reliability has been described for high frequencies such as $f_2 \geq$ 5 kHz (Wagner et al. 2008), $f_2 \geq$ 6 kHz (Reavis et al. 2015), and $f_2 \geq$ 8 kHz (Keppler et al. 2010). Low test-retest reliability at frequencies above 8 kHz may be associated with calibration errors due to different probe placements in the ear canal (Charaziak & Shera 2017). In the present study, for f_2 = 4 to 10 kHz, the test-retest differences of L_{OD} correlated moderately with the test-retest differences of calibration levels, but for higher frequencies f_2 = 11 to 14 kHz the correlation decreased. Thus, calibration errors may only explain part of the variability of L_{OD} in the mid frequencies and an even smaller part of the variability at higher frequencies. The trend for poorer test-retest reliability at higher frequencies is also described in studies using advanced calibration techniques with average ADs between 3 and 4 dB for f_2 = 12 to 16 kHz, as for example in Dreisbach et al. (2018) and Maxim et al. (2019).

In the present study, a statistically significant increase of test-retest reliability of L_{OD}, $L_{DP}(t)$, and r^2 at higher stimulus levels L_2 was not found for all f_2 (1 to 14 kHz) and L_2 (25 to 80 dB SPL), although in general, the test-retest reliability of these metrics appeared to increase at higher stimulus levels. The most consistent observations were (1) the test-retest reliability of $L_{DP}(t)$ was approximately independent of L_2 up to 3 kHz, and (2) the test-retest reliability of r^2 tended to increase with increasing L_2 for frequencies up to 11 kHz. An inhomogeneous dependence of the test-retest reliability on L_2 has been described in the literature without consistent dependence on L_2 (Franklin et al. 1992) and with varying degrees (Beattie & Bleech 2000; Wagner et al. 2008; Stuart et al. 2009; Keppler et al. 2010; Maxim et al. 2019). When recording a DPOAE at a low stimulus level L_2, the concomitant low DPOAE response with a low-SNR may be compromised by the noise floor, which may impact on the detection of the DPOAE signal (Whitehead et al. 1993) and, therefore, may result in low test-retest reliability.

In the present experiments, one explanation for an inconsistent relationship between L_2 and the DPOAE test-retest reliability might be that optimal L_1, L_2 stimulus-level pairs were not used at some stimulus frequencies in some subjects. Suboptimal stimulus-level pairs can eventuate if an online DPOAE map were to have been classified as invalid. Then, since the optimal level parameters were sought only in the first session, suboptimal pairs are likely to have been carried over to the subsequent sessions. As another possibility, although remote in normal-hearing subjects, suboptimal values might have developed in later sessions due to changes in middle-ear transmission.

Comparison with the Literature

Comparisons with other studies should be viewed with reservations due to differences in experimental design. Supplementary Table 2 in Supplemental Digital Content, http://links.lww.com/EANDH/B413, provides exemplary studies and a review of repeated DPOAE measurements.

For example, in the study of Beattie et al. (2003), the test-retest reliability of DPOAE levels was determined using the "standard error of measurement" (SEM) to calculate the 95% confidence interval based on measurements made twice within 10 days using continuously applied stimulus tones for f_2 = 500 Hz to 4 kHz in 50 normal-hearing subjects. For the short-term test-retest reliability, their data suggest that differences between two DPOAE measurements must exceed 7 dB at 1 to 4 kHz to be considered clinically abnormal and, therefore, requiring further clarifying diagnostics. The data of the present study (L_{OD}) would suggest, in comparison to the study of Beattie et al., based on the range of ADs for f_2 = 1 to 4 kHz, that a 5-dB test-retest difference warrants further evaluation (4.72 dB for 90% data range and 6.12 dB for 95% data range). A study by Wagner et al. (2008), using continuously applied stimulus-level combinations chosen according to the algorithm of Kummer et al. (1998), describes mean ADs of 1.0 dB (SD = 1.4 dB) for f_2 = 1 to 6 kHz and L_2 = 20 to 60 dB in immediate re-measurements with the ear-probe left in place, and of 2.3 dB (SD = 2.5 dB) when the probe was reinserted within 10 days. In comparison, the present study (L_{OD}) showed mean ADs of 2.38 dB (SD = 2.23 dB) for f_2 = 1 to 6 kHz and L_2 = 20 to 60 dB SPL, where the probe was reinserted for each session and the test-retest time difference ranged from 8 hr to 3 months.

Maxim et al. (2019) described mean ADs between 1 and 3.6 dB for the nonlinear-distortion component of DPOAE, using swept tones for f_2 = 0.626 to 16 kHz and L_1/L_2 = 55/40 and 65/65 dB SPL/dB SPL, based on three test sessions within 3 months for five subjects. In the present study, the mean of the ADs for L_{OD} ranged from 1.74 to 3.85 dB for f_2 = 1 to 14 kHz and L_2 = 40 and L_2 = 65 dB SPL (the L_2 values used by Maxim et al. [2019]), based on seven test sessions over 3 months in 20 ears. The study of Maxim et al. is of special interest as it relies on a swept-tone method to remove the influence of the DPOAE coherent-reflection component and, furthermore, averages DPOAE sweep data across 1/3 octave in order to calculate an AD. Moreover, it uses an advanced calibration technique, whereas in the present study an SPL-calibration, although corrected by an artificial ear, was used. There is an additional key difference between both studies; namely, the measurement time to record one DPOAE to calculate an AD differs: For the study of Maxim et al., we estimate an averaging time of 35 s per DPOAE level, whereas our study required approximately

2.5 s to record a single DPOAE signal.* Therefore, in an effort to compare the test-retest reliability of both methods extracting the nonlinear-distortion component, but without taking calibration issues into account, we chose mean ADs at f_2 = 1 to 3 kHz and moderate levels of L_2 = 65 dB SPL from Maxim et al. that amount to approximately 1 dB, in comparison to the mean AD for the same stimulus conditions in the present study with 1.84 dB (SD = 1.88 dB). Moreover, averaging four moderate DPOAE levels at a single f_2 with an SNR above 15 dB, improved the test-retest reliability further to a mean AD of 1.25 dB (SD = 1.01 dB) or median AD of 0.99 dB. In other words, the two techniques can yield similar test-retest reliabilities, but with considerably shorter measurement times in the case of our short-pulse algorithm.

Thus, seen from a technical viewpoint, the algorithm used for the extraction of L_{OD} based on short-pulse stimulation proved to perform with high reliability, especially considering the short measurement time of 2.5 s to record one DPOAE signal. While the extraction of the nonlinear-distortion component appeared to provide similar test-retest reliability as reported in the literature for conventional stimulus paradigms, it does offer more detailed information on the functional state of the cochlear amplifier from one tonotopic region. Conventional continuous stimuli cause pronounced interference effects between DPOAE components of similar size. Then, assuming that both components are in quadrature or counter phase and undergo with time slightly different amplitude and/or phase changes, one can imagine that the test-retest differences of a DPOAE signal containing both components might increase. On the one hand, in normal-hearing subjects, our results based on the reproducibility metric of the time course of the DPOAE-envelope pressure, r^2, with median > 0.97 at all f_2 and L_2 (Fig. 5), suggest that the relative amplitudes and phases of the DPOAE components remain stable over a period of at least 3 months. On the other hand, in patients, pathology might impact the interference state of the two DPOAE components and, therefore, differential information on the time course of both DPOAE components may become important in future clinical studies.

*In Maxim et al. (2019), OAE measurement time for one session comprising test blocks A and B was reported to be approximately 40 min, with a short break of 5 to 10 min between blocks A and B. Thus, we estimate that OAE measurement time for one block required 20 min, and the time between two measurements of the same condition was 30 min (time per block plus break). Within one block, eight conditions were tested (DPOAE, SFOAE, different calibration methods, two levels), reducing the measurement time for one condition to 2.5 min or 150 s. Dividing by 13 frequencies, the measurement time per DPOAE level to calculate one AD would be 11.5 s. Then, Maxim et al. presented three sweeps serving different frequency bands simultaneously. Therefore, the measurement time for collecting one DPOAE level to calculate one AD is estimated to be 34.5 s (the underlying assumption being that measurement time was allocated equally to SFOAEs and DPOAEs). For the present study, using short-pulse stimulation, the measurement time required at one DPOAE level to obtain an AD was (only) approximately 2.5 s (depending on frequency, cf. Material and methods). Note that for a multi-frequency short-pulsed stimulus paradigm, the possibility of measuring sufficiently wide-spaced frequency bands simultaneously, as did Maxim et al., is generally straightforward to implement. However, when doing so, possible masking effects must be ruled out meticulously, especially for unfavorable hearing-loss configurations.

Value of Advanced DPOAE Techniques for Clinical Application and Research

In clinical settings, DPOAEs are primarily utilized as a rapid test for assessing cochlear function, offering a dichotomous diagnosis of cochlear impairment. However, these standard DPOAE protocols are generally confined in their frequency range and exhibit limited specificity and sensitivity, making them susceptible to false positives (Gorga et al. 1997; Zelle et al. 2017a). In research, considerable progress has been achieved through the development of advanced DPOAE techniques, aimed at providing a more accurate and comprehensive assessment of cochlear function and its relation to underlying pathologic conditions. Unlike conventional continuous tones used in clinical routine, DPOAE techniques in research settings often use stimuli specifically designed to align with the sound processing capabilities of cochlear mechanics, such as chirps or tone pulses. Advanced measurement paradigms typically incorporate extended protocols that scan the cochlea using multiple variations of stimulus parameters (Poling et al. 2019; Stiepan et al. 2022), combine stimulus frequency otoacoustic emission (SFOAE) and DPOAE measurements (Abdala et al. 2021; Stiepan et al. 2023), use enhanced calibration techniques (Charaziak & Shera 2017; Maxim et al. 2019; Abdala et al. 2022; Garastro et al. 2023), utilize specific signal-processing methods, such as time-frequency decomposition (Moleti et al. 2012) or use least-squares fitting to mathematical models (Long et al. 2008).

Although various studies have yielded promising results, the adaption of advanced methods from laboratory to clinical practice has been quite limited to date. For instance, enhanced calibration techniques and the use of swept-tone or pulsed DPOAEs are not widely accessible to audiologists and physicians; they are predominantly available only through specialized scientific measurement equipment. One major reason for this slow transition may be attributed to the increased measurement time that accompanies current advanced DPOAE techniques. For instance, pulsed DPOAE stimulation inherently has a reduced duty cycle as compared with continuous-tone stimulation. Swept-tone DPOAE techniques expand the measured stimulus-frequency space by filling in information between the audiometric frequencies customarily used clinically. These characteristics inevitably compete against time-efficiency requirements of clinical and outpatient routines.

To address these challenges and the shortage of suitable medical devices, several research groups have been continuously refining advanced DPOAE measurement paradigms. These enhancements aim to increase efficiency while also providing a deeper insight into cochlear mechanics. For instance, recent developments in swept-tone DPOAE protocols have enabled DPOAE recordings up to 20 kHz (Stiepan et al. 2022). In addition, significant reductions in measurement times have been achieved by concurrently presenting chirps at multiple frequency pairs (Glavin et al. 2023).

Similarly, pulsed DPOAEs have evolved from a creative tool initially developed to determine signal onset and latency (Whitehead et al. 1996) and to examine or reduce the DPOAE fine structure (Talmadge et al. 1999; Vetešník et al. 2009; Zelle et al. 2017b). They have now become an efficient paradigm that enables the analysis of DPOAE growth without the artifacts typically resulting from two-source interference (Zelle et al. 2015), significantly decreasing the error of EDPTs when related to

behavioral thresholds in normal-hearing and hearing-impaired subjects (Dalhoff et al. 2013; Zelle et al. 2017c).

This advancement has been facilitated by using binaural short stimulus pulses in pulse trains and automated analysis of DPOAE time signals, as demonstrated in the present study. This approach enables efficient DPOAE source separation, reducing measurement time to 6 min for binaural recording of 140 DPOAEs per ear. For currently used clinical DPOAE test protocols, which involve a much smaller stimulus space, this equates to a measurement duration of approximately 30 to 60 s. Further measurement-time reductions are possible through the simultaneous presentation of multiple frequency pairs and tailoring SNR requirements to specific clinical tasks. In addition, the discrete nature of pulsed stimuli facilitates the use of adaptive frequency- and level-scanning techniques, which can further decrease the number of DPOAEs required for recording.

Pulsed DPOAEs are a versatile tool for investigating the state of the cochlear amplifier, as they provide a comprehensive time course of the DPOAE, encompassing the two main DPOAE components and their state of interference. There have been promising reports indicating differential effects on both DPOAE components in relation to pathological conditions, such as endolymphatic hydrops (Stiepan et al. 2023) and ototoxic (Poling et al. 2019) or noise-induced cochlear damage (Poling et al. 2022). Furthermore, pulsed DPOAEs provide additional insights through the parameters r^2 and L_{OD}, as introduced in the present study. The current algorithm could be augmented by DPOAE latency measurements, which are directly derivable from the short-pulse DPOAE time course. Latency has been shown to convey information about the frequency selectivity of auditory signal processing (Sumner et al. 2018), and might well turn out to become a useful predictor of speech recognition deficits in the future. In general, a multimodal analysis that incorporates multiple parameters relating to the functional state of the cochlear amplifier could potentially reduce the risk of misleading diagnostic information. This is particularly relevant in serial monitoring, such as during ototoxic treatment or in the course of regenerative therapy.

The already validated achievements of advanced DPOAE techniques in research, such as pulsed DPOAE or swept-tone DPOAE, yield enhanced accuracy and separation of the two major OAE generation processes. The enhanced accuracy reduces the likelihood of erroneous clinical conclusions about the functional state of the cochlea. Furthermore, together with the potential of future validations of differential diagnostic capabilities by gathering independent information on both OAE sources—for example, the level dependence of their amplitudes and latencies—make it highly probable that the one or the other technique will enter the clinical stage soon. What remains to be addressed, however, is the development or choice of sufficiently efficient protocols tailored to specific clinical pathologies, and their validation in large patient groups.

CONCLUSION

The results of the present study support our hypothesis that pulsed DPOAE time signals show a high test-retest reliability for (1) the nonlinear-distortion component level L_{OD}, (2) the time course of the DPOAE-envelope levels $L_{DP}(t)$, and (3) the squared, zero-lag correlation coefficient (r^2) between time courses of the DPOAE-envelope pressures measured in two sessions. To date, there is no international standard on how to use DPOAE in serial monitoring programs (Clemens et al. 2019). Establishing standard clinical DPOAE protocols for serial monitoring programs using large multicenter studies is complicated by the different stimulus parameters and DPOAE signal-processing techniques used in different clinics and research centers.

On the basis of the current state of the literature and with the knowledge gained from this study on the test-retest reliability of pulsed DPOAE timing signals, we propose a DPOAE protocol for future serial monitoring applications that takes into account the following factors: (1) separating the two main DPOAE components and if feasible representing their state of interference, (2) using individual optimal stimulus parameters, (3) realizing an SNR of at least 15 dB, (4) implementing a pressure calibration procedure that reduces calibration errors, (5) considering frequency-specific and if applicable level-dependent test-retest reliabilities and their corresponding reference ranges, and (6) focusing on stimulus levels L_2 that are as low as possible with sufficient SNR to capture the nonlinear functional state of the cochlear amplifier operating at its highest gain.

The pulsed DPOAE method is a very promising tool for serial monitoring as it not only can readily satisfy the earlier-mentioned requirements but also is time-efficiently applicable in patients. Pulsed DPOAE time signals provide the possibility of measuring at discrete points with respect to frequency which might make them more flexibly applicable as compared with, for example, chirp-evoked DPOAEs. Nevertheless, implementing automated and standardized DPOAE signal processing and component extraction based on pulsed DPOAE is a sophisticated task (Whitehead et al. 1996; Vetešník et al. 2009; Dalhoff et al. 2013; Zelle et al. 2020). However, pulsed DPOAE time signals simultaneously depict both principal components of the DPOAE signal—the nonlinear-distortion component and the coherent-reflection component. As emphasized by others (Abdala et al. 2022), information about changes in the time courses of these two components might improve their diagnostic value in serial screening for ascertaining the functional state of the cochlear amplifier in response to endogenous and exogenous factors. On the basis of the present results, it appears advantageous to consider r^2 simultaneously with the L_{OD}. Their use provides additional information about the functional state of the cochlear amplifier, which minimizes the risk of false negative/positive results regarding the question of whether there is an actual change in the functional state of the cochlear amplifier.

ACKNOWLEDGMENTS

The authors thank especially Dr. Lina Maria Serna Higuita for her support with statistics.

Linda Dierkes is currently at the Department of Medicine, Niels-Stensen-Kliniken Marienhospital Osnabrück, Osnabrück, Germany. Lore Helene Braun is currently at the Department of Radiooncology, Marienhospital Stuttgart, Stuttgart, Germany.

This work was supported by a Junior Clinician Scientist Sponsorship of the Faculty of Medicine of the Eberhard-Karls-University Tübingen to K.B. (No. 421-0-0) and the German Research Council, Grant No. DFG BA 7554/1-1. Advisory service in statistical methodology was provided by the Institute for Clinical Epidemiology and Applied Biometry of the University of Tübingen.

K.B. designed and performed experiments, analyzed the data, performed statistical analysis, and wrote the paper. E.D. reviewed data, provided interpretative analysis, critical revision, and edited the paper. L.D. performed experiments. L.H.B. designed the experiments. A.W.G. provided critical revision and edited the paper. D.Z. designed figures, developed the measurement setup, provided critical revision, and edited the paper. All authors discussed the results and implications and commented on the manuscript.

The authors have no conflicts of interest to disclose.

Address for correspondence: Katharina Bader, Department of Otolaryngology, Head and Neck Surgery, Eberhard-Karls-University Tübingen, Elfriede-Aulhornstraße 5, 72076 Tübingen, Germany. E-mail: katharina.bader@med.uni-tuebingen.de

Received August 27, 2023; accepted April 10, 2024; published online ahead of print May 29, 2024

REFERENCES

Abdala, C., & Kalluri, R. (2017). Towards a joint reflection-distortion otoacoustic emission profile: Results in normal and impaired ears. *J Acoust Soc Am*, *142*, 812–824.

Abdala, C., Luo, P., Shera, C. A. (2015). Optimizing swept-tone protocols for recording distortion-product otoacoustic emissions in adults and newborns. *J Acoust Soc Am*, *138*, 3785–3799.

Abdala, C., Luo, P., Shera, C. A. (2022). Characterizing the relationship between reflection and distortion otoacoustic emissions in normal-hearing adults. *J Assoc Res Otolaryngol*, *23*, 1–18.

Abdala, C., Ortmann, A. J., Guardia, Y. C. (2021). Weakened cochlear nonlinearity during human aging and perceptual correlates. *Ear Hear*, *42*, 832–845.

Avan, P., Büki, B., Maat, B., Dordain, M., Wit, H. P. (2000). Middle ear influence on otoacoustic emissions. I: Noninvasive investigation of the human transmission apparatus and comparison with model results. *Hear Res*, *140*, 189–201.

Avan, P., Büki, B., Petit, C. (2013). Auditory distortions: Origins and functions. *Physiol Rev*, *93*, 1563–1619.

Bader, K., Dierkes, L., Braun, L. H., Gummer, A. W., Dalhoff, E., Zelle, D. (2021). Test-retest reliability of distortion-product thresholds compared to behavioral auditory thresholds. *Hear Res*, *406*, 108232.

Beattie, R. C., & Bleech, J. (2000). Effects of sample size on the reliability of noise floor and DPOAE. *Br J Audiol*, *34*, 305–309.

Beattie, R. C., & Ireland, A. (2000). Effects of sample size on the noise floor and distortion product otoacoustic emissions. *Scand Audiol*, *29*, 93–102.

Beattie, R. C., Kenworthy, O. T., Luna, C. A. (2003). Immediate and short-term reliability of distortion-product otoacoustic emissions: Confiabilidad inmediata y a corto plazo de las emisiones otoacústicas por productos de distorsión. *Int J Audiol*, *42*, 348–354.

Boege, P., & Janssen, T. (2002). Pure-tone threshold estimation from extrapolated distortion product otoacoustic emission I/O-functions in normal and cochlear hearing loss ears. *J Acoust Soc Am*, *111*, 1810–1818.

Brownell, W. E. (1990). Outer hair cell electromotility and otoacoustic emissions. *Ear Hear*, *11*, 82–92.

Charaziak, K. K., & Shera, C. A. (2017). Compensating for ear-canal acoustics when measuring otoacoustic emissions. *J Acoust Soc Am*, *141*, 515–531.

Christensen, A. T., Ordoñez, R., Hammershøi, D. (2015). Stimulus ratio dependence of low-frequency distortion-product otoacoustic emissions in humans. *J Acoust Soc Am*, *137*, 679–689.

Clemens, E., van den Heuvel-Eibrink, M. M., Mulder, R. L., Kremer, C .M., Hudson, M. M., Skinner, R., Constine, L. S., Bass, J. K., Kuehni, C. E., Langer, T., van Dalen, E. C., Bardi, E., Bonne, N-X., Brock, P. R., Brooks, B., Carleton, B., Caron, E., Chang, K. W., Johnston, K., Kinght, K., et al. International Guideline Harmonization Group Ototoxicity Group. (2019). Recommendations for ototoxicity surveillance for childhood, adolescent, and young adult cancer survivors: A report from the International Late Effects of Childhood Cancer Guideline Harmonization Group in collaboration with the PanCare Consortium. *Lancet Oncol*, *20*, e29–e41.

Dalhoff, E., Turcanu, D., Vetešník, A., Gummer, A. W. (2013). Two-source interference as the major reason for auditory-threshold estimation error based on DPOAE input-output functions in normal-hearing subjects. *Hear Res*, *296*, 67–82.

Dreisbach, L. E., Long, K. M., Lees, S. E. (2006). Repeatability of high-frequency distortion-product otoacoustic emissions in normal-hearing adults. *Ear Hear*, *27*, 466–479.

Dreisbach, L. E., & Siegel, J. H. (2001). Distortion-product otoacoustic emissions measured at high frequencies in humans. *J Acoust Soc Am*, *110*, 2456–2469.

Dreisbach, L., Zettner, E., Chang Liu, M., Meuel Fernhoff, C., MacPhee, I., Boothroyd, A. (2018). High-frequency distortion-product otoacoustic emission repeatability in a patient population. *Ear Hear*, *39*, 85–100.

Durante, A. S., Shaheen Akhtar, U., Dhar, S. (2022). Distortion product otoacoustic emission component behavior as a function of primary frequency ratio and primary level. *Ear Hear*, *43*, 1824–1835.

Fausti, S. A., Helt, W. J., Phillips, D. S., Gordon, J. S., Bratt, G. W., Sugiura, K. M., Noffsinger, D. (2003). Early detection of ototoxicity using 1/6th-octave steps. *J Am Acad Audiol*, *14*, 444–450.

Franklin, D. J., McCoy, M. J., Martin, G. K., Lonsbury-Martin, B. L. (1992). Test/retest reliability of distortion-product. *Ear Hear*, *13*, 417–429.

Garasto, E., Stefani, A., Pierantozzi, M., Cerroni, R., Conti, M., Maranesi, S., Mercuri, N. B., Chiaravalloti, A., Schillaci, O., Viziano, A., Moleti, A., Sisto, R. (2023). Association between hearing sensitivity and dopamine transporter availability in Parkinson's disease. *Brain Commun*, *5*, fcad075.

Glavin, C. C., Dhar, S., Goodman, S. S. (2023). Measurement of swept level distortion product otoacoustic emission growth functions at multiple frequencies simultaneously. *JASA Express Lett*, *3*, 064401.

Go, N. A., Stamper, G. C., Johnson, T. A. (2019). Cochlear mechanisms and otoacoustic emission test performance. *Ear Hear*, *40*, 401–417.

Gorga, M. P., Neely, S. T., Dorn, P. A., Hoover, B. M. (2003). Further efforts to predict pure-tone thresholds from distortion product otoacoustic emission input/output functions. *J Acoust Soc Am*, *113*, 3275–3284.

Gorga, M. P., Neely, S. T., Ohlrich, B., Hoover, B., Redner, J., Peters, J. (1997). From laboratory to clinic: A large scale study of distortion product otoacoustic emissions in ears with normal hearing and ears with hearing loss. *Ear Hear*, *18*, 440–455.

Heitmann, J., Waldmann, B., Schnitzler, H.-U., Plinkert, P. K., Zenner, H.-P. (1998). Suppression of distortion product otoacoustic emissions (DPOAE) near 2f1−f2 removes DP-gram fine structure—Evidence for a secondary generator. *J Acoust Soc Am*, *103*, 1527–1531.

Helleman, H. W., & Dreschler, W. A. (2012). Overall versus individual changes for otoacoustic emissions and audiometry in a noise-exposed cohort. *Int J Audiol*, *51*, 362–372.

Jerger, J. (1970). Clinical experience with impedance audiometry. *Arch Otolaryngol*, *92*, 311–324.

Johnson, T. A., Neely, S. T., Kopun, J. G., Dierking, D. M., Tan, H., Gorga, M. P. (2010). Clinical test performance of distortion-product otoacoustic emissions using new stimulus conditions. Ear Hear, *31*, 74–83.

Kalluri, R., & Shera, C. A. (2001). Distortion-product source unmixing: A test of the two-mechanism model for DPOAE generation. *J Acoust Soc Am*, *109*, 622–637.

Keppler, H., Dhooge, I., Maes, L., D'Haenens, W., Bockstael, A., Philips, B., Swinnen, F., Vinck, B. (2010). Transient-evoked and distortion product otoacoustic emissions: A short-term test-retest reliability study. *Int J Audiol*, *49*, 99–109.

Keshishzadeh, S., Garrett, M., Verhulst, S. (2021). Towards personalized auditory models: Predicting individual sensorineural hearing-loss profiles from recorded human auditory physiology. *Trends Hear*, *25*, 2331216520988406.

Konrad-Martin, D., Knight, K., McMillan, G. P., Dreisbach, L. E., Nelson, E., Dille, M. (2020). Long-term variability of distortion-product otoacoustic emissions in infants and children and its relation to pediatric ototoxicity monitoring. *Ear Hear*, *41*, 239–253.

Kreitmayer, C., Marcrum, S. C., Picou, E. M., Steffens, T., Kummer, P. (2019). Subclinical conductive hearing loss significantly reduces otoacoustic emission amplitude: Implications for test performance. *Int J Pediatr Otorhinolaryngol*, *123*, 195–201.

Kummer, P., Janssen, T., Arnold, W. (1998). The level and growth behavior of the 2 f1−f2 distortion product otoacoustic emission and its relationship to auditory sensitivity in normal hearing and cochlear hearing loss. *J Acoust Soc Am*, *103*, 3431–3444.

Kummer, P., Janssen, T., Hulin, P., Arnold, W. (2000). Optimal L1−L2 primary tone level separation remains independent of test frequency in humans. *Hear Res*, *146*, 47–56.

Lapsley Miller, J. A., Marshall, L., Heller, L. M., Hughes, L. M. (2006). Low-level otoacoustic emissions may predict susceptibility to noise-induced hearing loss. *J Acoust Soc Am*, *120*, 280–296.

Laurell, G., & Bagger-Sjöbäck, D. (1991). Dose-dependent inner ear changes after i.v. administration of cisplatin. *J Otolaryngol*, *20*, 158–167.

Long, G. R., Talmadge, C. L., Lee, J. (2008). Measuring distortion product otoacoustic emissions using continuously sweeping primaries. *J Acoust Soc Am*, *124*, 1613–1626.

Marshall, L., Lapsley Miller, J. A., Heller, L. M., Wolgemuth, K. S., Hughes, L. M., Smith, S. D., Kopke, R. D. (2009). Detecting incipient inner-ear damage from impulse noise with otoacoustic emissions. *J Acoust Soc Am*, *125*, 995–1013.

Mauermann, M., & Kollmeier, B. (2004). Distortion product otoacoustic emission (DPOAE) input/output functions and the influence of the second DPOAE source. *J Acoust Soc Am*, *116*, 2199–2212.

Maxim, T., Shera, C. A., Charaziak, K. K., Abdala, C. (2019). Effects of forward- and emitted-pressure calibrations on the variability of otoacoustic emission measurements across repeated probe fits. *Ear Hear*, *40*, 1345–1358.

McMillan, G. P. (2014). On reliability. *Ear Hear*, *35*, 589–590.

Mills, M. L., Shen, Y., Withnell, R. H. (2021). Examining the factors that contribute to non-monotonic growth of the 2f1–f2 otoacoustic emission in humans. *J Assoc Res Otolaryngol*, *22*, 275–288.

Moleti, A., Longo, F., Sisto, R. (2012). Time-frequency domain filtering of evoked otoacoustic emissions. *J Acoust Soc Am*, *132*, 2455–2467.

Moleti, A., Sisto, R., Tognola, G., Parazzini, M., Ravazzani, P., Grandori, F. (2005). Otoacoustic emission latency, cochlear tuning, and hearing functionality in neonates. *J Acoust Soc Am*, *118*, 1576–1584.

Petersen, L., Wilson, W. J., Kathard, H. (2017). A systematic review of stimulus parameters for eliciting distortion product otoacoustic emissions from adult humans. *Int J Audiol*, *56*, 382–391.

Poling, G. L., Siegel, J. H., Lee, J., Dhar, S. (2022). The influence of self-reported noise exposure on 2$f1$-$f2$ distortion product otoacoustic emission level, fine structure, and components in a normal-hearing population. *J Acoust Soc Am*, *151*, 2391–2402.

Poling, G. L., Vlosich, B., Dreisbach, L. E. (2019). Emerging distortion product otoacoustic emission techniques to identify preclinical warning signs of basal cochlear dysfunction due to ototoxicity. *Appl Sci*, *9*, 3132.

Prieve, B. A., Thomas, L., Long, G., Talmadge, C. (2020). Observations of distortion product otoacoustic emission components in adults with hearing loss. *Ear Hear*, *41*, 652–662.

Rao, A., & Long, G. R. (2011). Effects of aspirin on distortion product fine structure: Interpreted by the two-source model for distortion product otoacoustic emissions generation. *J Acoust Soc Am*, *129*, 792–800.

Reavis, K. M., McMillan, G., Austin, D., Gallun, F., Fausti, S. A., Gordon, J. S., Helt, W. J., Konrad-Martin, D. (2011). Distortion-product otoacoustic emission test performance for ototoxicity monitoring. *Ear Hear*, *32*, 61–74.

Reavis, K. M., McMillan, G. P., Dille, M. F., Konrad-Martin, D. (2015). Meta-analysis of distortion product otoacoustic emission retest variability for serial monitoring of cochlear function in adults. *Ear Hear*, *36*, e251–e260.

Roede, J., Harris, F. P., Probst, R., Xu, L. (1993). Repeatability of distortion product otoacoustic emissions in normally hearing humans. *Audiology*, *32*, 273–281.

Scheperle, R. A., Neely, S. T., Kopun, J. G., Gorga, M. P. (2008). Influence of in situ, sound-level calibration on distortion-product otoacoustic emission variability. *J Acoust Soc Am*, *124*, 288–300.

Schilder, A. G. M., Su, M. P., Blackshaw, H., Lustig, L., Staecker, H., Lenarz, T., Safieddine, S., Gomes-Santos, C. S., Holme, R., Warnecke, A. (2019). Hearing protection, restoration, and regeneration: An overview of emerging therapeutics for inner ear and central hearing disorders. *Otol Neurotol*, *40*, 559–570.

Shehata-Dieler, W. E., Dieler, R., Klagges, T., Moser, L. M. (1999). Intra- and intersubject variability of acoustically evoked otoacoustic emissions. II. Distortion product otoacoustic emissions. *Laryngorhinootologie*, *78*, 345–350.

Shera, C. A., & Guinan, J. J. (1999). Evoked otoacoustic emissions arise by two fundamentally different mechanisms: A taxonomy for mammalian OAEs. *J Acoust Soc Am*, *105*, 782–798.

Shibata, S. B., West, M. B., Du, X., Iwasa, Y., Raphael, Y., Kopke, R. D. (2020). Gene therapy for hair cell regeneration: Review and new data. *Hear Res*, *394*, 107981.

Stavroulaki, P., Apostolopoulos, N., Segas, J., Tsakanikos, M., Adamopoulos, G. (2001). Evoked otoacoustic emissions—An approach for monitoring cisplatin induced ototoxicity in children. *Int J Pediatr Otorhinolaryngol*, *59*, 47–57.

Stiepan, S., Goodman, S. S., Dhar, S. (2022). Optimizing distortion product otoacoustic emission recordings in normal-hearing ears by adopting cochlear place-specific stimuli. *J Acoust Soc Am*, *152*, 776–788.

Stiepan, S., Shera, C. A., Abdala, C. (2023). Characterizing a joint reflection-distortion OAE profile in humans with endolymphatic hydrops. *Ear Hear*, *44*, 1437–1450.

Stuart, A., Passmore, A. L., Culbertson, D. S., Jones, S. M. (2009). Test–retest reliability of low-level evoked distortion product otoacoustic emissions. *J Speech Lang Hear Res*, *52*, 671–681.

Sumner, C. J., Wells, T. T., Bergevin, C., Sollini, J., Kreft, H. A., Palmer, A. R., Oxenham, A. J., Shera, C. A. (2018). Mammalian behavior and physiology converge to confirm sharper cochlear tuning in humans. *Proc Natl Acad Sci U S A*, *115*, 11322–11326.

Talmadge, C. L., Long, G. R., Tubis, A., Dhar, S. (1999). Experimental confirmation of the two-source interference model for the fine structure of distortion product otoacoustic emissions. *J Acoust Soc Am*, *105*, 275–292.

Vetešník, A., Turcanu, D., Dalhoff, E., Gummer, A. W. (2009). Extraction of sources of distortion product otoacoustic emissions by onset-decomposition. *Hear Res*, *256*, 21–38.

Wagner, W., Heppelmann, G., Vonthein, R., Zenner, H. P. (2008). Test–retest repeatability of distortion product otoacoustic emissions. *Ear Hear*, *29*, 378–391.

Whitehead, M. L., Lonsbury-Martin, B. L., Martin, G. K. (1993). The influence of noise on the measured amplitudes of distortion-product otoacoustic emissions. *J Speech Hear Res*, *36*, 1097–1102.

Whitehead, M. L., Stagner, B. B., Martin, G. K., Lonsbury-Martin, B. L. (1996). Visualization of the onset of distortion-product otoacoustic emissions, and measurement of their latency. *J Acoust Soc Am*, *100*, 1663–1679.

Whitehead, M. L., Stagner, B. B., McCoy, M. J., Lonsbury-Martin, B. L., Martin, G. K. (1995). Dependence of distortion-product otoacoustic emissions on primary levels in normal and impaired ears. II. Asymmetry in L1,L2 space. *J Acoust Soc Am*, *97*, 2359–2377.

Zelle, D., Bader, K., Dierkes, L., Gummer, A. W., Dalhoff, E. (2020). Derivation of input-output functions from distortion-product otoacoustic emission level maps. *J Acoust Soc Am*, *147*, 3169–3187.

Zelle, D., Dalhoff, E., Gummer, A. W. (2017a). Objective audiometry with DPOAEs: New findings for generation mechanisms and clinical applications. *HNO*, *65*, 122–129.

Zelle, D., Dalhoff, E., Gummer, A. W. (2017b). Comparison of time-domain source-separation techniques for short-pulse distortion-product otoacoustic emissions. *J Acoust Soc Am*, *142*, EL544–EL548.

Zelle, D., Lorenz, L., Thiericke, J. P., Gummer, A. W., Dalhoff, E. (2017c). Input-output functions of the nonlinear-distortion component of distortion-product otoacoustic emissions in normal and hearing-impaired human ears. *J Acoust Soc Am*, *141*, 3203–3219.

Zelle, D., Thiericke, J. P., Dalhoff, E., Gummer, A. W. (2015). Level dependence of the nonlinear-distortion component of distortion-product otoacoustic emissions in humans. *J Acoust Soc Am*, *138*, 3475–3490.

Zhao, F., & Stephens, D. (1999). Test-retest variability of distortion-product otoacoustic emissions in human ears with normal hearing. *Scand Audiol*, *28*, 171–178.